Systematics in the Enthalpies of Formation of Anhydrous Aluminosilicate Zeolites, Glasses, and Dense Phases

Alexandra Navrotsky* and Zheng-Rong Tian[a]

Keywords: aluminosilicate · enthalpy · glasses · thermodynamics · zeolites

Introduction

Aluminosilicate zeolites consist of microporous continuous frameworks of linked AlO_4 and SiO_4 tetrahedra, with the negative framework charge balanced by cations in one or more sites within the cages. Within a given framework type, compositional variation can be represented by the charge coupled ionic substitution:

$$Si^{4+} = Al^{3+} + (1/n)M^{n+} \quad (1)$$

As products of hydrothermal synthesis in nature, the laboratory, or industry, zeolites contain hydrated cations, and their chemical formula can be expressed, per mol of tetrahedra, as:

$$\text{Hydrated zeolite} \mathrel{\hat{=}} M^{n+}_{x/n}Al_xSi_{1-x}O_2 \cdot mH_2O \quad (2)$$

The extent of aluminum substitution ranges from $x = 0$ to $x = 0.5$. The major cations are the alkali and alkaline earths. Writing the formula per mol of tetrahedra allows ready comparison of zeolites having different numbers of tetrahedra per crystallographic unit cell and emphasizes that zeolites are derivatives of silica structures through the charge balanced "stuffing" substitution above. Many zeolites can be dehydrated without framework collapse; this constitutes "activation" for many catalytic processes. The anhydrous zeolite has the formula, per tetrahedral unit:

$$\text{Anhydrous zeolite} = M^{n+}_{x/n}Al_xSi_{1-x}O_2 \quad (3)$$

Zeolites can also be ion exchanged. Thus, once a specific structure is synthesized at a given Al/(Al + Si) ratio, a number of different hydrated and/or anhydrous zeolites containing various cations are accessible. Variation in the initial synthesis conditions produces different framework types and aluminum contents. Therefore a whole series of materials showing systematic compositional variation within a given structure has been available for physical property measurements, and, especially over the last five years, for the determination of heats of formation by high temperature oxide melt solution calorimetry.[1] The thermodynamics of formation provides important insight into phase equilibria, mineralogical parageneses, optimum synthesis conditions, and the driving forces for synthesis and transformation. However, because not all structures are tolerant of dehydration and because thermochemical measurements are tedious and require excellent sample quality, the data set for the energetics of zeolite formation is far from complete.

The energetics of anhydrous framework aluminosilicate glasses showing analogous charge coupled substitution [Eq. (1)] have been studied extensively.[2] Thermochemical data for dense framework aluminosilicates (phases such as the feldspars and the stuffed silica derivatives including nepheline, kalsilite, and eucryptite) are also available.[3] The enthalpies of many silica polymorphs (dense frameworks, glass, and a number of zeolites) have been reported.[4] The enthalpies of formation of about twenty anhydrous aluminosilicate zeolites are known.[5]

The purpose of this paper is to bring together the thermochemical data for the charge coupled substitution [Eq. (1)] in glasses, anhydrous zeolites, and dense aluminosilicates to form a systematic and predictive model for the enthalpies of formation of anhydrous aluminosilicate zeolites. We consider the dependence of the energetics on framework type, aluminum content, and charge balancing cation and define a set of linear equations describing the enthalpies of formation. This model for anhydrous aluminosilicate zeolites will be incorporated, in a subsequent paper, into a predictive model for the thermodynamics of hydrated zeolites.

Thermochemical Trends in Glasses

Roy and Navrotsky[6] reported the enthalpies of solution of a number of framework aluminosilicate glasses (M = Li, Na, K,

[a] Prof. A. Navrotsky, Dr. Z.-R. Tian
Thermochemistry Facility
Department of Chemical Engineering and Materials Science
University of California at Davis
One Shields Avenue, Davis, CA 95616 (USA)
Fax: (+1) 530-752-9307
E-mail: anavrotsky@ucdavis.edu

Rb, Cs, Mg, Ca, Sr, Ba, Pb) in molten $2\,PbO \cdot B_2O_3$ near 973 K (see Table 1). The enthalpies of solution become more endothermic (glasses energetically more stable) with increasing aluminum content, reaching a maximum near $x = Al/(Al + Si) = 0.5$. These data can be used to calculate the enthalpy of formation of the glass from its binary oxide components at 298 K, $\Delta H_{f,298\,K,oxides}$:

$$x M_{x/n}O_{2n/2}\,(crystal) + (x/2)Al_2O_3\,(corundum) + (1-x)SiO_2\,(quartz) = M_{x/n}Al_xSi_{1-x}O_2\,(glass) \quad (4)$$

The results are shown in Table 1 and Figure 1a. For $0 < x < 0.5$, the Al/(Al + Si) ratios of interest for zeolites, $\Delta H_{f,298\,K,oxides}$ varies linearly with x and defines a fan of straight lines whose slope becomes steeper (greater energetic stabilization) in the order Pb, Mg, Ca, Li, Sr, Ba, Na, K, Rb, Cs. This stabilization can be related to the ionic potential (z/r = charge/radius) and the extent to which the charge-balancing cation is able to perturb the tetrahedral framework.[7]

Comparison of Zeolites, Dense Phases, and Glasses

Petrovic et al.[4] determined the enthalpies of six zeolitic silicas relative to quartz. These data have been augmented by recent work by Piccione et al.[8] It is striking that the enthalpies of all SiO_2 zeolites measured span a range of only about 7 kJ mol^{-1} and overlap the value of silica glass. These zeolite enthalpies lie 8–13 kJ mol^{-1} above the enthalpy of quartz at 298 K. The significance of these small enthalpies and their weak dependence on framework type has been discussed previously.[4, 8]

A major question is whether the energetics of different zeolite structure types and glass are similarly close to each other at other compositions, that is, for a given Al/(Al + Si) ratio and charge-balancing cation M. Tables 2 and 3 and Figures 1b–c summarize the available data. The enthalpies of formation from oxide components at 298 K of the dense frameworks and of the anhydrous zeolites form fans of lines very similar to those for the glasses.

The slopes of these lines, for dense phase, zeolite, and glass, are plotted versus ionic potential (charge/radius = z/r) in Figure 2. The data show a trend of increasing stabilization (more negative slope) with decreasing ionic potential (greater basicity of the oxide of the extra-framework cation). This is consistent with the model proposed by Navrotsky et al.[7] for glasses, in which the electrostatic stabilization caused by the charge coupled substitution [Eq. (1)] is offset by the perturbation of the framework by high field strength cations.

The trends for specific extra-framework cations are compared for dense frameworks, zeolites, and glasses in Figure 3a–d. For M = Li (Figure 3a), the sparse zeolite data refer to the faujasite structure (FAU), a relatively open framework with 12-membered rings (see Table 4). The zeolites are somewhat higher than the glasses in enthalpy, which in turn are above the dense frameworks. The data for the dense aluminosilicate phases are numerous and well constrained because the stuffed β-quartz $Li_xAl_xSi_{1-x}O_2$ phase forms an essentially continuous solid solution.[3b] The lines for dense phase, glass, and zeolite are parallel.

For M = Na (Figure 3b), the zeolite data are far more numerous than for other cations. Two groups of zeolites can be identified: those with 12-membered rings (and more open

Table 1. Enthalpies of solution of aluminosilicate glasses in $2\,PbO \cdot B_2O_3$ at 973 K and their enthalpies of formation from crystalline oxides at 298 K kJ mol^{-1}. A mol is defined as a formula unit containing one mol of tetrahedra, that is, $M_{x/n}Al_xSi_{1-x}O_2$.

Cation type	x = Al/(Al + Si)	$\Delta H_{sol,973\,K}$[a] [kJ mol^{-1} TO_2]	$\Delta H_{f,973\,K,oxides}$[b] [kJ mol^{-1} TO_2]	$\Delta H_{f,298\,K,oxides}$[c] [kJ mol^{-1} TO_2]
M = Li	0.0	− 4.30 ± 0.20	7.00 ± 1.05	9.10 ± 2.33
	0.1	− 5.35 ± 0.61	− 0.95 ± 0.63	− 0.28 ± 0.67
	0.2	− 3.23 ± 0.57	− 3.73 ± 0.59	− 3.74 ± 0.63
	0.25	− 1.18 ± 0.22	− 6.44 ± 0.28	− 6.50 ± 0.33
	0.40	4.04 ± 0.67	− 13.66 ± 0.70	− 13.69 ± 0.74
M = Na	0.0	− 4.30 ± 0.20	7.00 ± 1.05	9.10 ± 2.33
	0.125	− 2.65 ± 0.14	− 3.32 ± 0.23	− 8.11 ± 0.31
	0.188	0.95 ± 0.17	− 7.75 ± 0.24	− 15.80 ± 0.27
	0.25	5.00 ± 0.07	− 12.62 ± 0.18	− 23.88 ± 0.29
	0.25	–[e]	–[e]	− 24.60 ± 1.21[d]
	0.33	11.05 ± 0.13	− 19.74 ± 0.22	− 35.15 ± 0.32
	0.42	16.53 ± 0.12	− 26.42 ± 0.22	− 46.49 ± 0.34
	0.50	–[e]	–[e]	− 66.50 ± 2.09[a]
M = K	0.0	− 4.30 ± 0.20	7.00 ± 1.05	9.10 ± 2.33
	0.05	− 6.00 ± 0.16	− 3.79 ± 0.25	− 0.16 ± 0.30
	0.125	0.62 ± 0.17	− 18.63 ± 0.25	− 14.05 ± 0.30
	0.188	7.32 ± 0.16	− 32.24 ± 0.24	–25.72 ± 0.30
	0.212	7.32 ± 0.09	− 34.87 ± 0.20	–30.16 ± 0.30
	0.25	11.64 ± 0.22	− 43.36 ± 0.28	− 37.24 ± 0.30
	0.25	–[e]	–[e]	− 42.50 ± 1.33[d]
	0.40	19.82 ± 0.10	− 68.00 ± 0.21	− 64.98 ± 0.30
M = Rb	0.0	− 4.30 ± 0.20	7.00 ± 1.05	9.10 ± 2.33
	0.100	− 1.15 ± 0.43	− 17.40 ± 0.47	− 15.10 ± 0.42
M = Cs	0.0	− 4.30 ± 0.20	7.00 ± 1.05	9.10 ± 2.33
	0.100	0.85 ± 0.22	− 14.17 ± 0.29	− 14.19 ± 0.36
M = Mg	0.0	− 4.30 ± 0.20	7.00 ± 1.05	9.10 ± 2.33
	0.113	− 11.41 ± 0.18	10.00 ± 1.01	11.38 ± 1.09
	0.341	− 9.97 ± 0.23	14.40 ± 1.82	15.05 ± 1.85
	0.565	− 8.91 ± 0.34	19.08 ± 1.30	19.06 ± 1.43
M = Ca	0.0	− 4.30 ± 0.20	7.00 ± 1.05	9.10 ± 2.33
	0.10	− 9.31 ± 0.15	1.97 ± 0.26	4.53 ± 0.32
	0.16	− 8.55 ± 0.10	− 0.62 ± 0.25	3.64 ± 0.29
	0.25	− 6.36 ± 0.16	− 5.36 ± 0.33	1.24 ± 0.32
	0.34	− 5.71 ± 0.11	− 8.93 ± 0.39	0.37 ± 0.31
	0.38	− 4.44 ± 0.14	− 11.42 ± 0.43	− 1.00 ± 0.33
	0.42	− 3.67 ± 0.05	− 13.40 ± 0.45	− 1.86 ± 0.31
	0.50	–[e]	–[e]	− 7.75 ± 1.19
M = Sr	0.0	− 4.30 ± 0.20	7.00 ± 1.05	9.10 ± 2.33
	0.10	− 9.51 ± 0.85	− 2.07 ± 0.89	2.60 ± 0.90
	0.20	− 7.46 ± 0.84	− 11.40 ± 0.94	− 2.04 ± 0.91
	0.25	− 4.83 ± 0.66	− 17.67 ± 0.84	− 5.96 ± 0.76
	0.35	− 2.13 ± 0.55	− 27.65 ± 0.90	− 11.27 ± 0.73
M = Ba	0.0	− 4.30 ± 0.20	7.00 ± 1.05	9.10 ± 2.33
	0.10	− 8.78 ± 0.84	− 6.21 ± 0.92	− 4.17 ± 0.89
	0.15	− 7.05 ± 0.71	− 13.29 ± 0.88	− 10.21 ± 0.77
	0.25	− 2.07 ± 0.75	− 28.96 ± 1.13	− 23.83 ± 0.81
	0.35	2.80 ± 0.64	− 44.52 ± 1.33	− 37.54 ± 0.73
M = Pb	0.0	− 4.30 ± 0.20	7.00 ± 1.05	9.10 ± 2.33
	0.10	− 9.07 ± 0.98	7.20 ± 0.99	7.02 ± 1.02
	0.15	− 7.04 ± 1.70	6.38 ± 1.71	6.13 ± 1.72
	0.35	− 4.22 ± 0.72	5.99 ± 0.74	7.82 ± 0.77
	0.45	− 1.21 ± 0.11	5.41 ± 0.19	7.07 ± 0.31

[a] Data from ref. [6]. [b] Calculated using heats of solution of binary oxides measured in this laboratory. [c] Calculated using heat contents of crystals and glasses. [d] Data from ref. [3a]. [e] Different methodology used, values in this column not measured.

0947-6539/01/0704-0770 $ 17.50+.50/0 *Chem. Eur. J.* **2001**, *7*, No. 4

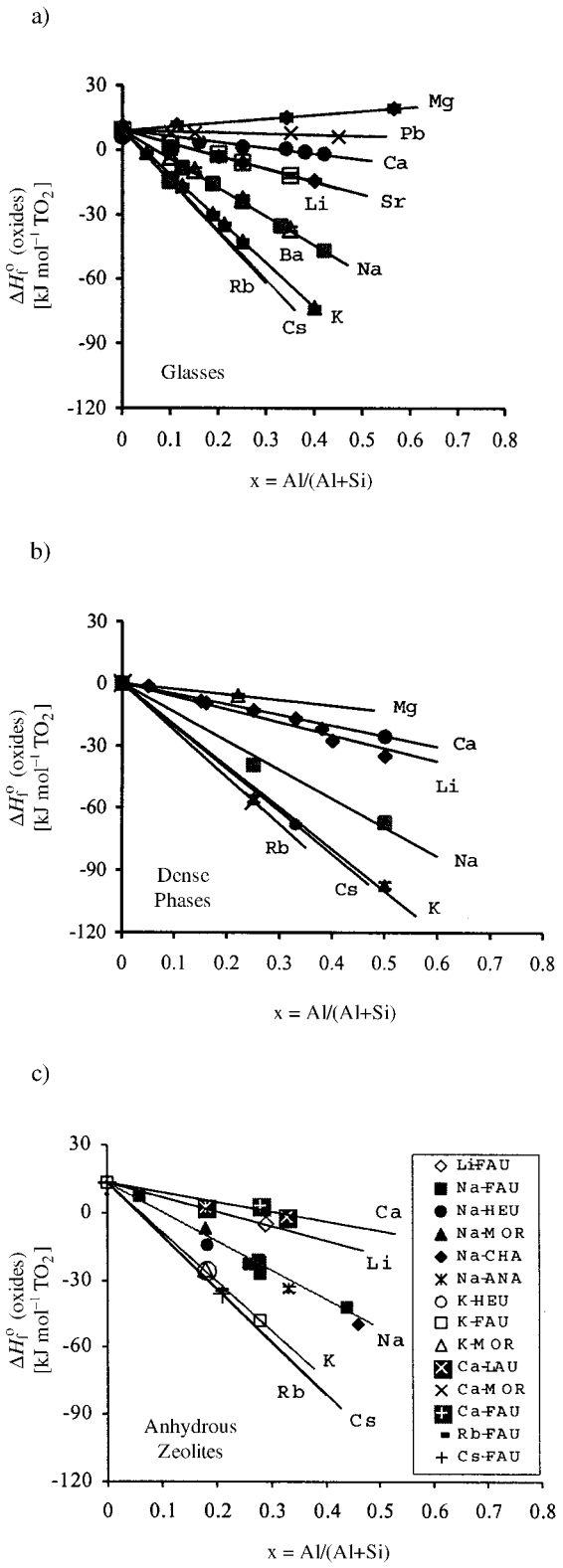

Figure 1. Enthalpies of formation at 298 K from the oxides as a function of $x = \mathrm{Al}/(\mathrm{Al}+\mathrm{Si})$ for a) all glasses; b) all dense phases, and c) all zeolites.

structures) in the FAU and MOR framework types, which lie somewhat above glass in enthalpy, and those with 8- and 10-membered rings (and denser structures) in the HEU, ANA, and CHA framework types, which lie at essentially the same enthalpy as the corresponding glass. For pure SiO_2 frameworks, the data show similar trends, with MFI and MEL very close to glass in enthalpy and FAU distinctly higher (see Table 4 and discussion in Petrovic et al.[4]). For the purposes of modeling of enthalpies of formation below, we will distinguish these two groups of zeolites (12-membered rings versus 8- and 10-membered rings). For M = K (Figure 3c), there are not enough data for the zeolites to distinguish their trend from that of glass. Similar trends are obtained from the limited number of data points for M = Cs and M = Rb (Figures 3d, 3e). For M = Ca (Figure 3f), the zeolite data are dominated by values for those with 8- and 10-membered rings, and fall on top of the glass data.

Table 2. Enthalpies of formation from the oxides at 298 K of dense framework aluminosilicates, per mol of tetrahedra.

Phase	Composition	$x =$ Al/(Al + Si)	$\Delta H_{f,298\,K,oxides}^0$ [kJ mol^{-1} TO$_2$]
stuffed quartz[a]	$Li_{0.50}Al_{0.50}Si_{0.50}O_2$	0.05	-0.59 ± 0.66
stuffed quartz[a]	$Li_{0.50}Al_{0.50}Si_{0.50}O_2$	0.15	-8.10 ± 0.42
stuffed quartz[a]	$Li_{0.50}Al_{0.50}Si_{0.50}O_2$	0.16	-8.94 ± 0.47
stuffed quartz[a]	$Li_{0.50}Al_{0.50}Si_{0.50}O_2$	0.25	-13.14 ± 0.98
stuffed quartz[a]	$Li_{0.50}Al_{0.50}Si_{0.50}O_2$	0.33	-17.04 ± 0.56
stuffed quartz[a]	$Li_{0.50}Al_{0.50}Si_{0.50}O_2$	0.38	-22.47 ± 0.74
stuffed quartz[a]	$Li_{0.50}Al_{0.50}Si_{0.50}O_2$	0.40	-27.61 ± 0.83
stuffed quartz[a]	$Li_{0.50}Al_{0.50}Si_{0.50}O_2$	0.50	-34.89 ± 0.69
albite (low)[b]	$Na_{0.25}Al_{0.25}Si_{0.75}O_2$	0.25	-39.41 ± 1.01
nepheline[b]	$Na_{0.50}Al_{0.50}Si_{0.50}O_2$	0.50	-67.20 ± 2.04
microcline[b]	$K_{0.25}Al_{0.25}Si_{0.75}O_2$	0.25	-55.76 ± 1.27
kalsilite[b]	$K_{0.50}Al_{0.50}Si_{0.50}O_2$	0.50	-97.28 ± 1.74
Rb-microcline[c]	$Rb_{0.25}Al_{0.25}Si_{0.75}O_2$	0.25	-56.76 ± 0.30
pollucite[d]	$Cs_{0.33}Al_{0.33}Si_{0.67}O_2$	0.33	-68.10 ± 0.60
cordierite[b]	$Mg_{0.22}Al_{0.44}Si_{0.56}O_2$	0.22	-5.96 ± 0.16
anorthite[b]	$Ca_{0.25}Al_{0.50}Si_{0.50}O_2$	0.50	-25.45 ± 0.79
quartz[b]	SiO_2	0.00	0.00

[a] Data from ref. [3b]. [b] Data from ref. [3a]. [c] Data calculated from ref. [6]. [d] Data from ref. [10].

Table 3. Measured and predicted enthalpies of formation of anhydrous zeolites at 298 K, per mol of tetrahedra.

x[a]	Structure[b]	Formula	$\Delta H_{f\,(oxides)}^0$ [kJ mol^{-1} TO$_2$] (measured)	(predicted)	(Δ)[c]
0.292	Li-FAU[d]	$Li_{0.212}Na_{0.062}Ca_{0.001}Al_{0.292}Si_{0.709}O_2$	-5.24 ± 0.46	-5.2 ± 0.5	0.0
0.180	Na-MOR[e]	$Na_{0.180}Al_{0.180}Si_{0.820}O_2$	-6.46 ± 0.40	-9.8 ± 0.9	-3.3
0.256	Na-FAU[f]	$Na_{0.256}Al_{0.256}Si_{0.744}O_2$	-22.66 ± 1.00	-19.5 ± 1.1	3.2
0.280	Na-FAU[d]	$Na_{0.28}Al_{0.28}Si_{0.72}O_2$	-21.32 ± 0.59	-22.6 ± 1.2	-1.3
0.280	Na-FAU[e]	$Na_{0.280}Al_{0.280}Si_{0.72}O_2$	-22.06 ± 0.56	-22.6 ± 1.2	-0.5
0.285	Na-FAU[f]	$Na_{0.285}Al_{0.285}Si_{0.715}O_2$	-26.64 ± 1.00	-23.2 ± 1.2	3.4
0.444	Na-FAU[f]	$Na_{0.444}Al_{0.444}Si_{0.556}O_2$	-41.79 ± 1.00	-43.5 ± 1.7	-1.7
0.182	Na-HEU[e]	$Na_{0.182}Al_{0.182}Si_{0.818}O_2$	-14.11 ± 0.45	-16.2 ± 1.8	-2.1
0.333	Na-ANA[g]	$Na_{0.333}Al_{0.333}Si_{0.667}O_2$	-33.82 ± 1.37	-37.2 ± 2.4	-3.4
0.459	Na-CHA[h]	$Na_{0.459}Al_{0.459}Si_{0.541}O_2$	-49.47 ± 15.9	-54.7 ± 3.0	-5.2
0.182	Na-HEU[e]	$Na_{0.098}K_{0.085}Al_{0.182}Si_{0.818}O_2$	-20.86 ± 0.74	-22.0 ± 1.3	1.1
0.182	Na-HEU[e]	$Na_{0.110}K_{0.048}Ca_{0.012}Al_{0.182}Si_{0.818}O_2$	-13.43 ± 0.64	-16.8 ± 1.2	-3.4
0.180	K-MOR[e]	$K_{0.180}Al_{0.180}Si_{0.820}O_2$	-25.25 ± 0.57	-28.1 ± 1.8	-2.9
0.280	K-FAU[d]	$K_{0.26}Na_{0.02}Al_{0.28}Si_{0.72}O_2$	-48.03 ± 0.72	-48.7 ± 2.3	-0.7
0.182	K-HEU[e]	$K_{0.182}Al_{0.182}Si_{0.818}O_2$	-26.50 ± 0.48	-28.5 ± 1.8	-2.0
0.200	Rb-FAU[d]	$Rb_{0.20}Na_{0.06}Al_{0.28}Si_{0.72}O_2$	-34.34 ± 0.54	-34.3 ± 0.5	0.0
0.280	Cs-FAU[d]	$Cs_{0.21}Na_{0.07}Al_{0.28}Si_{0.72}O_2$	-36.09 ± 0.46	-36.1 ± 0.5	0.0
0.180	Ca-MOR[e]	$Ca_{0.090}Al_{0.180}Si_{0.820}O_2$	2.49 ± 0.40	3.8 ± 1.3	1.3
0.280	Ca-FAU[d]	$Ca_{0.14}Al_{0.28}Si_{0.72}O_2$	-3.41 ± 0.53	0.8 ± 1.5	4.2
0.180	Ca-MOR[e]	$Ca_{0.056}Na_{0.068}Al_{0.180}Si_{0.820}O_2$	-5.94 ± 0.66	-3.7 ± 1.0	2.2
0.333	Ca-LAU[i]	$Ca_{0.167}Al_{0.333}Si_{0.667}O_2$	-1.26 ± 1.11	-0.7 ± 1.6	0.6

[a] $x = \mathrm{Al}/(\mathrm{Al}+\mathrm{Si})$. [b] Three-letter symbol denotes zeolite structure, see ref. [11]. [c] Δ (difference) = (predicted value from the model) – (measured value). [d] Data from ref. [5e]. [e] S. Yang, A. Navrotsky, unpublished results. [f] Data from ref. [5c]. [g] Data from ref. [3a]. [h] Data from ref. [5d]. [i] Data from ref. [5a].

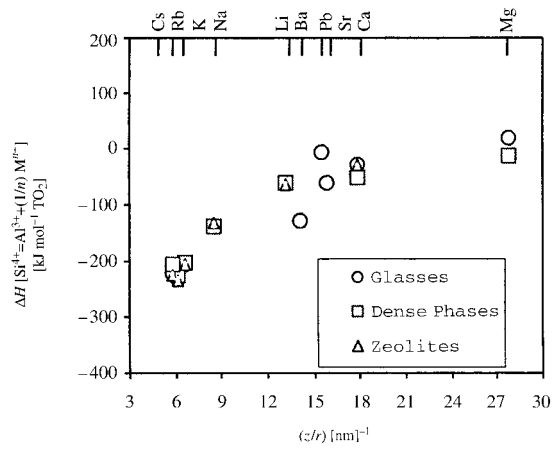

Figure 2. Enthalpies of substitution, $Si^{4+} \rightarrow Al^{3+} + (1/n)M^{n+}$ for glasses, dense phases, and zeolites as a function of the ionic potentials (z/r).

Table 4. Structural characteristics of zeolites and measured energetics of pure SiO_2 frameworks.

Structure	Symbol[a]	Pore[a] [Å]	Ring [number of tetrahedra]	$\Delta H_{(\text{relative to quartz})}$[b] [kJ mol^{-1} TO_2]
faujasite	FAU	7.4	12	13.1 ± 0.4
X	FAU	7.4	12	–[c]
Y	FAU	7.4	12	13.1 ± 0.4
mordenite	MOR	7.0×6.5	12	–[c]
clinoptilolite	HEU	7.6×3.0	10	–[e]
ZSM-5	MFI	5.6×5.3	10	8.2 ± 0.8
ZSM-11	MEL	5.4×5.3	10	8.2 ± 1.0
leonhadite	LAU	5.3×4.0	10	–[c]
Chabazite	CHA	3.8×3.8	8	–[c]
Analcime	ANA	4.2×1.6	8	–[e]
glass[f]	–[d]	–[d]	6 (mainly)	9.1 ± 1.5

[a] See ref. [11]. [b] Average used in model for the 12-membered ring is 13.1 ± 0.4; for 8- and 10-membered rings is 9.1 ± 1.5, and glass is 9.1 ± 1.5 kJ mol^{-1}. [c] Data not available. [d] Not defined.

The linear trends in $\Delta H_{\text{f,298 K,oxides}}$ were fitted numerically. In each case,

$$\Delta H_{\text{f,298 K,oxides}}\ [\text{kJ mol}^{-1}\ TO_2] = A + Bx \qquad (5)$$

where A is the intercept (for pure SiO_2) and B is the slope. For each type of aluminosilicate phase (dense phase, glass, 8- and 10-membered ring zeolite, 12-membered ring zeolite), we fitted all data simultaneously to linear equations. Thus, the value of A was fitted to be constant for each structural group. The parameter A depends on the structure and the parameter B depends on the nature of the cation. The method used in the linear regression takes both the error of each data point and the scatter of all data points from the line into consideration to generate the uncertainties for each A and B.[9] The results listed in Table 5 show that B is indeed the same for dense framework, zeolite, and glass of a given cation. The parameter A is zero for dense frameworks (quartz as the oxide reference state), 9.1 kJ mol^{-1} for glass (silica glass relative to quartz), 13.1 kJ mol^{-1} for 12-membered ring zeolites, and 9.1 kJ mol^{-1} for 8- and 10-membered ring zeolites (see Table 5). The parameter B is -63 kJ mol^{-1} for Li, -139 kJ mol^{-1} (for 8- and 10-membered rings) and -127 kJ mol^{-1} (for 12-membered rings) for Na, -206 kJ mol^{-1} for K, and about -30 kJ mol^{-1} for Ca [dense phase (ordered anorthite) excluded]. Data solely for the glasses define B for Rb, Ca, Mg, Ba, and Pb.

Prediction of Enthalpies of Formation of Anhydrous Aluminosilicate Zeolites

Equation (5) and the systematics above enable the prediction of the enthalpies of formation of any anhydrous aluminosilicate zeolite based on the correlation between the linear trends for each cation shown in Figure 3 and the parameters shown in Table 5. The results are included in Table 3. The predicted values are almost all within 3 kJ mol^{-1} of the measured ones. Part of the scatter almost certainly arises because the measured anhydrous zeolites are not all of equal quality. It is difficult to maintain both an intact framework and a totally anhydrous state in such materials. The scatter in measured data generally gives rise to an uncertainty of ± 0.4 to ± 0.8 kJ mol^{-1} for a given sample.

The generally good agreement between predicted and measured values suggests that this model can be used to predict enthalpies of formation of dehydrated zeolites of structures and compositions that either have not been measured or can not be made. These could include other framework types and cationic substitutions. The systematics predict that Mg- and Pb-substituted zeolite frameworks are of very limited stability but that those containing the larger alkalis (Rb and Ca) and alkaline earths (Sr and Ba) should have considerable energetic stability, as is seen for the glasses (see Table 5).

The next step in developing this model is to apply it to hydrated zeolites. For these an enthalpy of hydration must be added to the terms relating to structure, cation type, and aluminum content. Since many more hydrated zeolites than dehydrated zeolite frameworks are attainable, these hydrated zeolites will offer a more extensive test of the systematics developed in the study.

Acknowledgements

This work was supported by the National Science Foundation (DMR 97–31782). We thank Mr. J. Majzlan at the University of California, Davis for help in data analysis.

[1] a) A. Navrotsky, *Phys. Chem. Miner.* **1977**, *2*, 89–104; b) A. Navrotsky, *Phys. Chem. Miner.* **1997**, *24*, 222–241.

[2] a) A. Navrotsky, R. Hon, D. F. Weill, D. J. Henry, *Geochim. Cosmochim. Acta* **1980**, *44*, 1409–1423; b) A. Navrotsky, G. Peraudeau, P. McMillan, J.-P. Coutures, *Geochim. Cosmochim. Acta* **1982**, *46*, 2039–2047; c) A. Navrotsky, H. D. Zimmermann, R. L. Hervig, *Geochim. Cosmochim. Acta* **1983**, *47*, 1535–1538; d) R. L. Hervig, A. Navrotsky, *Geochim. Cosmochim. Acta* **1984**, *48*, 513–522; e) J. F. Stebbins, D. F. Weill, I. S. E. Carmichael, L. K. Moret, *Contrib. Mineral. Petrol.* **1982**, *80*, 276–284; f) P. Richet, Y. Bottinga, *Geochim. Cosmochim. Acta* **1984**, *48*, 453–470; g) J. F. Stebbins, I. S. E. Carmichael, L. K. Moret, *Contrib. Mineral. Petrol.* **1984**, *86*, 131–148.

[3] a) R. A. Robie, B. S. Hemingway, *Thermodynamic Properties of Minerals and Related Substances at 298.15 K and 1 bar (105 Pascals) Pressure and at Higher Temperatures*, U.S. Geological Survey Bulletin

0947-6539/01/0704-0772 $ 17.50+.50/0 *Chem. Eur. J.* **2001**, *7*, No. 4

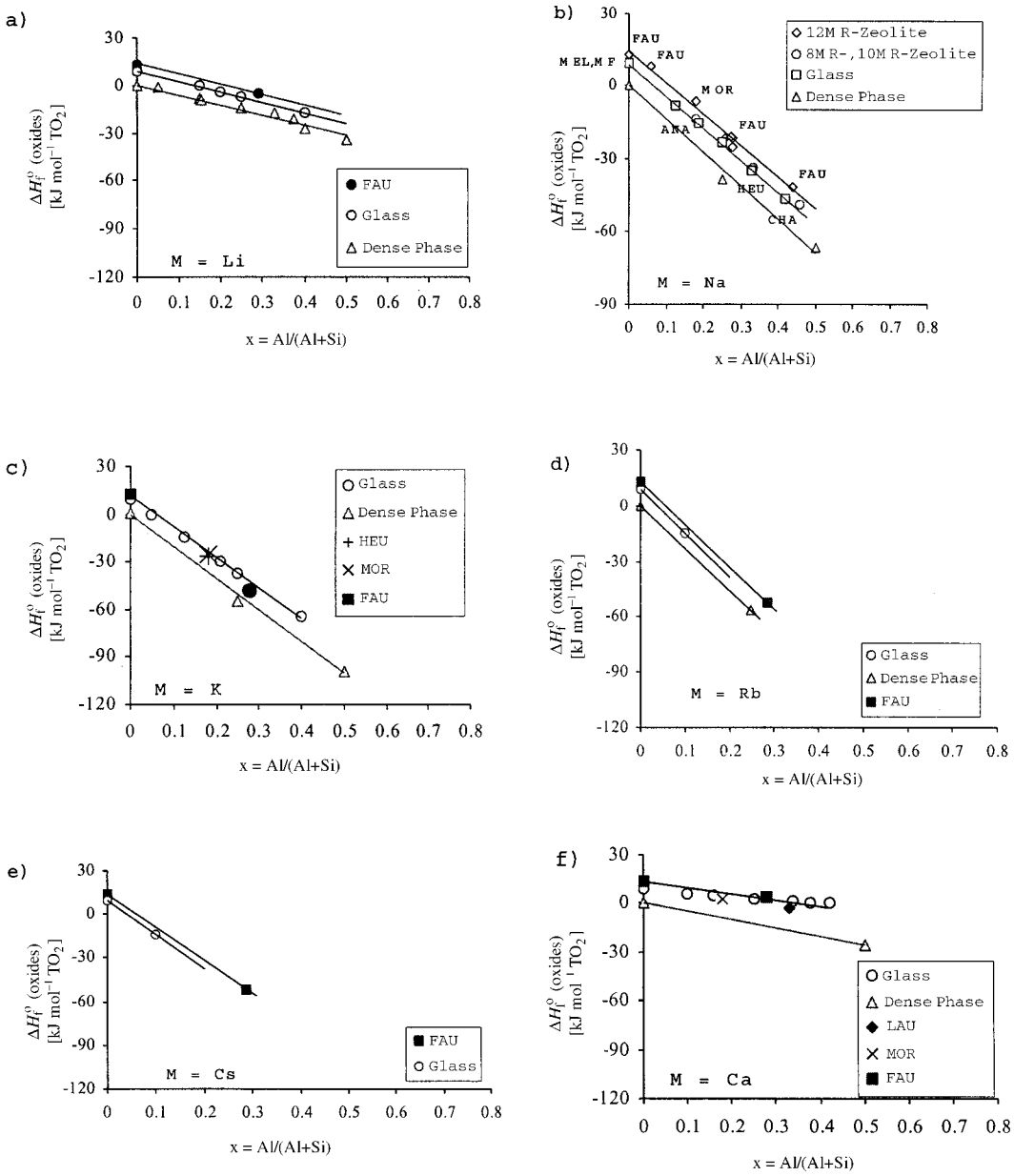

Figure 3. Comparison of the enthalpies of formation at 298 K from the oxides as a function of $x = \mathrm{Al}/(\mathrm{Al}+\mathrm{Si})$ for dense phases, glasses, and zeolites of a given cation: a) Li, b) Na, c) K, d) Rb, e) Cs, and f) Ca.

Table 5. Parameters for calculating enthalpies of formation at 298 K from the oxides as a function of $x = \mathrm{Al}/(\mathrm{Al}+\mathrm{Si})$, $\Delta H^0_{f\,(\mathrm{oxides})} = A + B \cdot x$, A, B in kJ mol^{-1} TO$_2$.

M	z/r	Glass[a]		Dense phase[b]		Zeolite[c]	
	[nm^{-1}]	A	B	A	B	A	B
Li	16.7	9.1 ± 1.5	-60.7 ± 5.4	0	-62.5 ± 2.1	13.1	-63.0[d]
Na	10.5	9.1 ± 1.5	-139 ± 5.6	0	-139 ± 4.9	9.1 ± 1.5	-139 ± 5.6[e]
		9.1 ± 1.5	-139 ± 5.6	0	-139 ± 4.9	13.1 ± 0.7	127.4 ± 3.4[f]
K	7.5	9.1 ± 1.4	-206.5 ± 6.6	0	-202 ± 5.2	9.1 ± 1.4	-206.5 ± 6.6[g]
Rb	6.8	9.1[d]	-233.0[d]	0	-227.0[d]	13.1[d]	-237.0[d]
Cs	5.9	9.1[d]	-223.9[d]	0	-206.4[d]	13.1[d]	-226.7[d]
Mg	30.1	9.1 ± 1.5	17.9 ± 4.1	0	-13.5[d]	–[i]	(18 ± 5)[h]
Ca	20.2	9.1 ± 1.1	29.5 ± 3.4	0	-50.9[d]	9.1 ± 1.1	-29.5 ± 3.4[g]
Sr	17.7	9.1 ± 1.6	-59.7 ± 6.3		–[i]	–[i]	(-60 ± 6)[h]
Ba	14.8	9.1 ± 1.6	-131.2 ± 7.0		–(i)	–(i)	(-132 ± 7)[h]
Pb	16.7	9.1 ± 1.4	-5.9 ± 3.9		–(i)	–(i)	(-6 ± 4)[h]

[a] Data from Figure 1a. [b] Data from Figure 1b. [c] Data from Figure 1c. [d] Based on only two points, error not defined; considered not reliable. [e] Data from Figure 3b with glasses and small ring (8- and 10-membered ring) zeolites fitted together. [f] Data from Figure 3b for large ring (12-membered ring) zeolites. [g] Glasses and zeolites fitted together. [h] Predicted from glass data. [i] Data not available.

  0947-6539/01/0704-0773 $ 17.50+.50/0

2131, **1995**, pp. 36–38; b) H. Xu, P. J. Heaney, A. Navrotsky, L. Topor, J. Liu, *Am. Mineral.* **1999**, *84*, 1360–1369.
[4] I. Petrovic, A. Navrotsky, M. E. Davis, S. I. Zones, *Chem. Mater.* **1993**, *5*,1805–1813.
[5] a) I. Kiseleva, A. Navrotsky, I. A. Belitsky, B. A. Fursenko, *Am. Mineral.* **1996**, *81*, 658–667; b) I. Kiseleva, A. Navrotsky, I. A. Belitsky, B. A. Fursenko, *Am. Mineral.* **1996**, *81*, 668–675; c) I. Petrovic, A Navrotsky, *Microporous Mater.* **1997**, *9*, 1–12; d) S. Shim, A. Navrotsky, T. R. Gaffney, J. E. MacMougall, *Am. Mineral.* **1999**, *84*, 1870–1882; e) S. Yang, A. Navrotsky, *Microporous Mesoporous Mater.* **2000**, *37*, 175–186; f) S. Yang, A. Navrotsky, unpublished results.
[6] B. N. Roy, A. Navrotsky, *J. Am. Ceram. Soc.* **1984**, *67*, 606–610.
[7] A. Navrotsky, K. L. Geisinger, P. McMillan, G. V. Gibbs, *Phys. Chem. Min.* **1985**, *11*, 284–298.
[8] P. M. Piccione, C. Laberty, S. Yang, M. A. Camblor, A. Navrotsky, M. E. Davis, *J. Phys. Chem. B*, in press.
[9] J. R. Tylor, *An Introduction to Error Analysis, the Study of Uncertainty in Physical Measurements*, Mill Valley, California University Science Books, **1982**.
[10] H. Xu, A. Navrotsky, M. L. Balmer, Y. Su, E. R. Bitten, unpublished results, **2000**.
[11] W. M. Meier, D. H. Olson, C. Baerlocher, *Atlas of Zeolite Structure Types*, 4th ed., Elsevier, **1996**, pp. 9–12.

0947-6539/01/0704-0774 $ 17.50+.50/0 *Chem. Eur. J.* **2001**, *7*, No. 4